Available online at www.sciencedirect.com
SCIENCE DIRECT®
Composites Science and Technology 66 (2006) 576–584
COMPOSITES SCIENCE AND TECHNOLOGY
www.elsevier.com/locate/compscitech

Fabrication and electromagnetic characteristics of electromagnetic wave absorbing sandwich structures

Ki-Yeon Park [a], Sang-Eui Lee [a], Chun-Gon Kim [a], Jae-Hung Han [a,*]

[a] *Department of Aerospace Engineering, Korea Advanced Institute of Science and Technology, 373-1 Guseong-dong, Yuseong-gu, Daejeon 305-701, Republic of Korea*

Received 30 July 2004; received in revised form 10 May 2005; accepted 24 May 2005
Available online 20 July 2005

Abstract

The radar absorbing structures (RAS) having sandwich structures in the X-band (8.2–12.4 GHz) frequencies were designed and fabricated. We added conductive fillers such as carbon black and multi-walled carbon nanotube (MWNT) to composite prepregs and polyurethane foams so as to efficiently increase the absorbing capacity of RAS. In order to improve the mechanical stiffness of RAS, we adopted the sandwich structures made of composite face sheets and foam cores. Glass fabric/epoxy composites containing conductive carbon black and carbon fabric/epoxy composites were used for the face sheets. Polyurethane foams containing MWNT were used as the core material. Their permittivity in the X-band was measured using the transmission line technique. The reflection loss characteristics for multi-layered sandwich structures were calculated using the theory of transmission and reflection in a multi-layered medium. Three kinds of specimens were fabricated and their reflection losses in the X-band were measured using the free space technique. Experimental results were in good agreement with simulated ones in 10-dB absorbing bandwidth.

Keywords: A. Fabrics/textiles; B. Electrical properties, Permittivity; Reflection loss; C. Sandwich, Radar absorbing structures

1. Introduction

The absorption and the interference shielding of electromagnetic wave have been very important issues for commercial and military purposes [1]. Electromagnetic interference (EMI) shielding problems are increasing in electronic and military communication owing to sensitive electronic devices and densely packed systems, so that the research on the EMI shielding has received more and more attention in recent years. On the other hand, the stealth technique is the most typical application of electromagnetic wave absorption technology. By reducing the detectability of aircrafts or warships, of which the radar cross-section (RCS) is a measure, they could evade radar detection, which affects not only the mission success rate but also survival of them in the hostile territory [2]. In fact, the stealth technique can be categorized into two methods. One is the shape optimization of the body so that incident electromagnetic wave can be scattered yielding minimum reflective wave. The other is the use of electromagnetic wave absorption materials and/or structures. In the early stage, many researchers mainly concentrated on the reduction of RCS and development of the radar absorbing materials (RAM), but nowadays investigation on the radar absorbing structures (RAS) using fiber-reinforced polymeric composite materials has received much attention [2].

Generally, electromagnetic wave absorption characteristics of material depend on its dielectric properties (the permittivity, ε), magnetic properties (the permeability, μ), thickness and frequency range. Dielectric

* Corresponding author. Tel.: +82 42 869 3723; fax: +82 42 869 3710.
E-mail address: jaehunghan@kaist.ac.kr (J.-H. Han).

0266-3538/$ - see front matter © 2005 Elsevier Ltd. All rights reserved.
doi:10.1016/j.compscitech.2005.05.034

composite absorbers depend on the ohmic loss of energy, which can be achieved by adding conductive fillers such as carbon black, graphite, or metal particles. On the other hand, magnetic composite absorbers are dependent on a kind of magnetic hysteresis effect, which is obtained when magnetic materials like ferrite are added to a matrix [3–5]. Of these two techniques, the magnetic composite absorber has two defects. First, density of the magnetic materials is too high to use them as a filler of absorbers. Second, the resonance frequency range showing effective characteristics exists in the MHz range. The efficiency of absorbers decreases rapidly in the GHz and beyond this range.

There are many kinds of electromagnetic absorbers. Salisbury screens and the Dallenbach layer are resonant absorbers in the narrow band frequency. There are also Jaumann absorbers of multi-layer structures and frequency selective surfaces (FSS) with reflection film as broadband absorbers in the broadband frequency [2,6,7].

One well-known application of electromagnetic wave absorbing sandwich structures is Visby Class corvette fabricated in Swedish Kockums [8]. It is designed to be virtually invisible in pursuit of hostile submarines and underwater mines for the Swedish Navy and the first vessel in the world to have fully developed stealth technology. Its hull consists of sandwich type fiber-reinforced composites, which are vinyl ester resin laminating a core of polyvinyl chloride (PVC) containing carbon fibers. It can be also used all the places where the reduction of the RCS such as a suction pipe and an air exhauster of aircrafts are needed.

This paper deals with design and fabrication of the RAS having sandwich structures in the X-band (8.2–12.4 GHz) frequencies. Glass fabric composites and polyurethane (PU) foams were used for the face sheets and the core, respectively. Carbon black and multi-walled carbon nanotube (MWNT) were used as conductive fillers. Their permittivity in the X-band was measured using the transmission line technique. The reflection loss characteristics for multi-layered sandwich structures were calculated. Three kinds of specimens were fabricated and their reflection losses in the X-band were measured using the free space technique. Experimental results were in good agreement with simulated ones in 10-dB absorbing bandwidth.

2. Electromagnetic wave absorber theory

2.1. Principle of single-layered electromagnetic wave absorber

Fig. 1 shows the single-layered electromagnetic wave absorber with thickness d. According to the transmission line theory, the input impedance at the surface of the absorber in Fig. 1 is

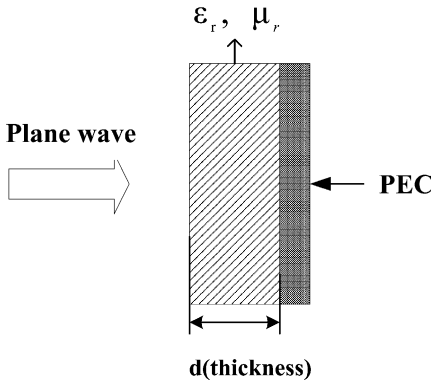

Fig. 1. Single-layered electromagnetic wave absorber.

$$Z_{\text{in}} = Z_0 \frac{Z_d + Z_0 \tanh \gamma d}{Z_0 + Z_d \tanh \gamma d}, \tag{1}$$

where the impedance of absorber material is $Z_0 = \sqrt{\mu/\varepsilon} = \sqrt{\mu_0 \mu_{\text{r}}/\varepsilon_0 \varepsilon_{\text{r}}}$ (ε_{r} is the relative permittivity) and the propagation constant γ is $\text{j}\omega\sqrt{\varepsilon\mu}$. Because the boundary back layer is the perfect electric conductor (PEC) in Fig. 1, the impedance at distance d, Z_d is zero. Thus, the input impedance becomes $Z_{\text{in}} = Z_0 \tanh \gamma d$. The impedance of air is $Z_{\text{a}} = \sqrt{\mu_0/\varepsilon_0}$ and the impedance matching condition minimizing reflection of incident wave is $Z_{\text{in}} = Z_{\text{a}}$. The normalized wave impedance $\widetilde{Z}$ for perpendicular incidence of plane wave is

$$\widetilde{Z} = \frac{Z_{\text{in}}}{Z_{\text{a}}} = \sqrt{\frac{\mu_{\text{r}}}{\varepsilon_{\text{r}}}} \tanh\left(\text{j}\frac{2\pi f d}{c}\sqrt{\mu_{\text{r}}\varepsilon_{\text{r}}}\right), \tag{2}$$

where ω is $2\pi f$ and the speed of light is $c = 1/\sqrt{\varepsilon_0 \mu_0}$ [9,10].

The condition minimizing reflection of incident plane wave is that $\widetilde{Z}$ is equal to 1. We call this state the impedance matching condition or the quarter lambda (wavelength) matching condition. The matching condition for multi-layered absorber is also the same case if effective normalized impedance for multi-layers is calculated.

2.2. Reflection and transmission in a multi-layered medium

A planar and inhomogeneous half-space with ε and μ varying as a function of z can be modeled by a multi-layered medium, where the electromagnetic property is piecewisely constant in each region (Fig. 2). The generalized reflection coefficient $\widetilde{R}_{i,i+1}$ at the interface between region i and $i+1$ considering whole structures can be written as

$$\widetilde{R}_{i,i+1} = R_{i,i+1} + \frac{T_{i,i+1}\widetilde{R}_{i+1,i+2}T_{i+1,i}\,\text{e}^{2\text{i}k_{i+1,z}(d_{i+1,}-d_i)}}{1 - R_{i+1,i}\widetilde{R}_{i+1,i+2}\,\text{e}^{2\text{i}k_{i+1,z}(d_{i+1,}-d_i)}}, \tag{3}$$

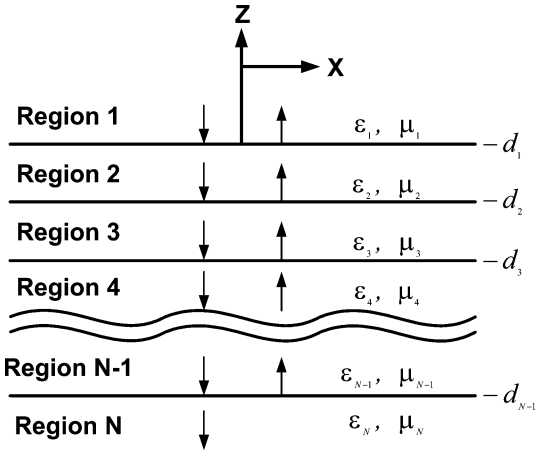

Fig. 2. Reflection and transmission in a multi-layered medium.

where $R_{i,i+1}$ is the reflection coefficient between region i and region $i+1$ considering only reflection between two regions. $T_{i,i+1}$ is the transmission coefficient between region i and region $i+1$. $k_{i,z}$ is the complex propagation constant in region i. d_i is the distance to region i. Eq. (3) can be simplified using $T_{ij} = 1 + R_{ij}$ and $R_{ij} = -R_{ji}$ as

$$\widetilde{R}_{i,i+1} = \frac{R_{i,i+1} + \widetilde{R}_{i+1,i+2}\, e^{2ik_{i+1,z}(d_{i+1,}-d_i)}}{1 + R_{i,i+1}\widetilde{R}_{i+1,i+2}\, e^{2ik_{i+1,z}(d_{i+1,}-d_i)}}. \tag{4}$$

These equations are recursive relations that express $\widetilde{R}_{i,i+1}$ in terms of $\widetilde{R}_{i+1,i+2}$ [11]. In this study, the reflection loss characteristics for multi-layered sandwich structures were obtained using the above equations.

3. Fabrication of absorbers and measurement of electromagnetic properties

3.1. Characteristics of sandwich structures

Sandwich construction has played increasingly important role in structural engineering because of its exceptionally high flexural stiffness-to-weight ratio compared to other constructions. Fig. 3 shows the cross-section of sandwich and monocoque construction.

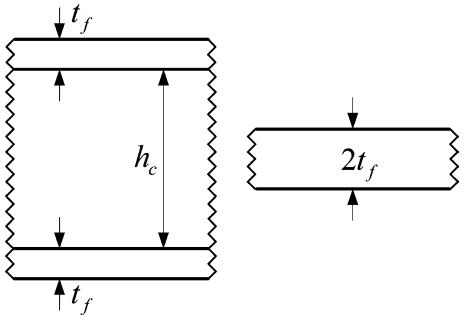

Fig. 3. Cross-section of sandwich and monocoque construction.

Eqs. (5) and (6) show the flexural stiffness (D) per unit width for monocoque and sandwich construction. It is assumed the core does not contribute to the flexural stiffness and $t_f/h_c \ll 1$, where E_f is the modulus of elasticity of isotropic face material, t_f and h_c are the thickness of face sheet and core and v_f is the Poisson's ratio of face sheet. If the thickness of foam core is 20 times as thick as that of face sheet, about 300 times gain in the flexural stiffness occurs.

$$D_{\text{mon.}} = \frac{E_f(2t_f)^3}{12(1-v_f^2)} = \frac{2E_f t_f^3}{3(1-v_f^2)},$$
$$D_{\text{sand.}} = \frac{2E_f t_f (h_c/2)^2}{1-v_f^2} = \frac{E_f t_f h_c^2}{2(1-v_f^2)}. \tag{5}$$

$$\frac{D_{\text{sand.}}}{D_{\text{mon.}}} = \frac{3}{4}\left(\frac{h_c}{t_f}\right)^2. \tag{6}$$

As a result, sandwich construction results in lower lateral deformations, higher buckling resistance and higher natural frequencies than do other constructions [12]. In this research, glass fabric/epoxy composites and carbon fabric/epoxy composites were used for the face sheets. Polyurethane foams were used for the core. Fig. 4 shows the schematics of sandwich construction fabricated in this study.

3.2. Fabrication of composite face sheets

Carbon black, Vulcan XC-72 by Cabot Carbon Ltd., were used as dielectric loss materials. Its specific gravity is 1.8 and the typical diameter is 27 nanometers. Glass fabric/epoxy prepreg, K618 supplied by Hankuk Fiber Co., was used for composite face sheets. The premixtures of epoxy matrix and carbon black were uniformly coated to the glass fabrics. Several prepregs with various carbon black contents were prepared. The weight percentages of carbon black with respect to total weight (epoxy resin, filler, diluent, carbon black and woven fiber) used to make composite prepreg were 0, 5, 6, 7 and 8 wt%. Conveniently, these specimens are indicated as CB0, CB5, CB6, CB7 and CB8, in this paper. When weight percentages of carbon black were less than 5 wt%, the dielectric loss were very low. When weight percentages of carbon black were more than 10 wt%, the specimen became electrically conductive with too high dielectric loss. There was also difficulty in fabrication owing to increasing viscosity. The layered specimens were fabricated by curing in the autoclave for 30 min at 80 °C and for 90 min at 130 °C, while stabilizing the pressure at 3 atm.

Carbon fabric/epoxy prepreg, CF3327 EPC supplied by Hankuk Fiber Co., was used for one composite face sheet showing shielding characteristics like conductor. Conveniently, these specimens are indicated as CFRP. These specimens were fabricated by curing in the

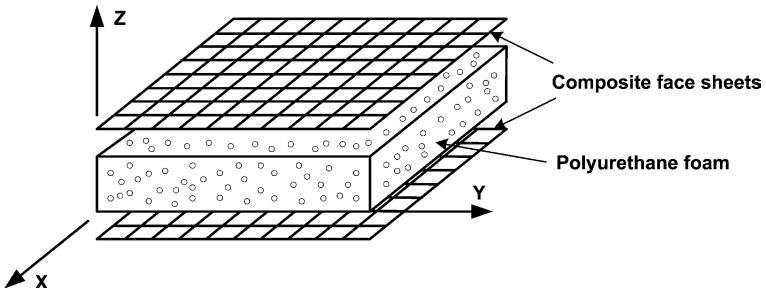

Fig. 4. Sandwich construction with composite face sheets and foam core.

autoclave for 30 min at 80 °C, 1.2 atm and for 2 h at 130 °C, 7 atm. The electric conductivity of these face sheets was about 10^4 S/m. We measured the surface resistivity using four-point probe and calculated the electrical conductivity [13]. The CFRP in RAS plays the same role as PEC to match impedance and the perfect reflection occurs in the CFRP.

3.3. Fabrication of polyurethane foam cores

Polyurethane (PU) is a polymer that is produced by the chemical reactions of the polyol and polyisocyanate. These can be produced as various kinds of foams such as soft, half-hard, hard, foaming and non-foaming foams according to component ratio of two constituent materials. PU foams have been widely used for mats in beds, seats in automobiles, sound absorbing materials, heat shield materials and building materials and so on.

In this research, we made hard PU foams using raw materials supplied by BASF Company Ltd. in Korea. We produced PU foams containing multi-walled carbon nanotube (MWNT) as another conductive filler in order to increase the permittivity of the foams. MWNT has higher conductivity than carbon black and their geometry such as high aspect ratio and small diameter has advantages of induction of permittivity. MWNT, CVD MWNT95 supplied by ILJIN Nanotech Co., were used in this study. Its diameter is 10–20 nm and specific surface area is 200 m^2/g.

The processing procedure of PU foams used as the core is prepared in three stages. First, the premixture was made by mixing blowing agent and catalyst with polyol. Second, another mixture was obtained by mixing MWNT with diphenylmethane diisocyanate (MDI) solution. The proportions of ingredients are as follows. The applied weight proportion of polyol, catalyst, MWNT and blowing agent are 79%, 0.2%, 20.8% and 0%. The weight proportions of this premixture and MDI are 20% and 80%. Lastly, these two solutions were mixed in the condition of 1500 rpm for 10 s using stirrer, and poured into a metal mold and allowed to cure for one day, so that PU foams containing MWNT were fabricated. The mold made of aluminium has the inner volume of $200 \times 200 \times 20$ mm and the thickness of 10 mm. The molding temperature is normal temperature. The weight percentages of MWNT contents in all constituent materials were 0, 3, and 5 wt%. As the weight percentages of MWNT contents exceeded 5 wt%, the solution was too viscous to be uniformly cured.

3.4. Measurement of electromagnetic characteristics for face sheets and foam cores

We prepared the *S*-parameter measurement system using the transmission line technique. The produced face sheets and foams were cut 22.86×10.16 mm in the size of WR 90 waveguide for X-band. Using network analyzer HP 8722ES and X-band waveguide, *S*-parameters of those specimens were measured. Permittivity of those specimens was calculated by using magnitude and phase of S_{21} among measured *S*-parameters. Figs. 5 and 6 show permittivity for glass fabric composites. As the weight percentage of carbon black contents increased in the composite, both real and imaginary parts of permittivity got larger. The imaginary part of permittivity for the CB0 was indicated zero and the increase of imaginary parts were remarkable when the weight percentage of carbon black contents were more than 5 wt%.

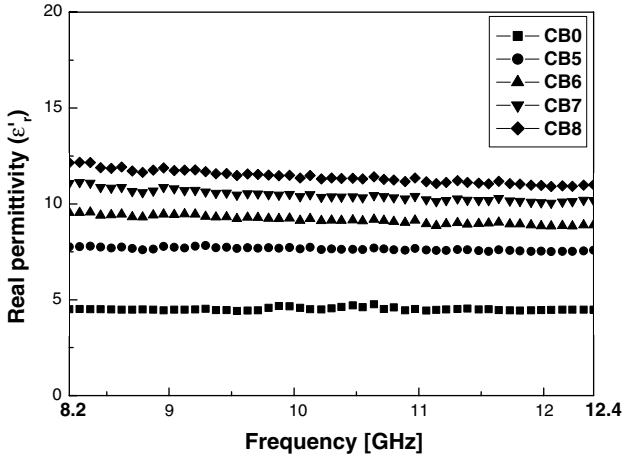

Fig. 5. Real part of permittivity vs. frequency for glass fabric composites.

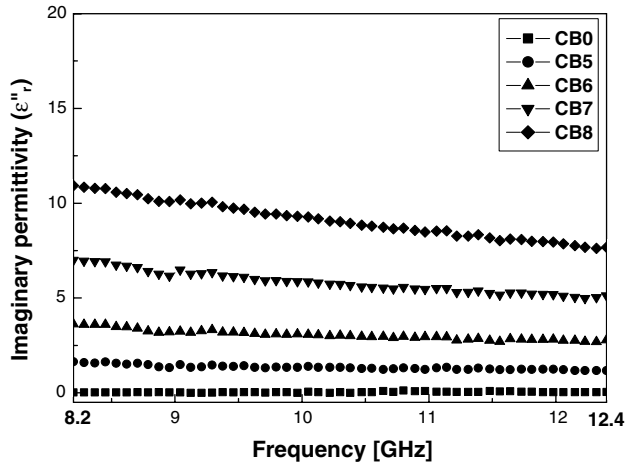

Fig. 6. Imaginary part of permittivity vs. frequency for glass fabric composites.

Table 1 shows MWNT weight percentage and density of PU foams in this study. Generally, densities of PU foams for half-hard and hard type are 60–120 kg/m^3. In this research, the densities of fabricated foams were a little higher than those of general PU foams because we fabricated PU foams in hard and non-forming type. The obtained permittivity for PU foams is shown in Fig. 7. The imaginary part of permittivity for Foam A is zero and the real part of permittivity for Foam A is indicated 1.2–1.3 times higher than that of vacuum. The imaginary part of permittivity for the case of Foam B and Foam C are approximately 0.1 and 0.3, respectively.

Table 1
MWNT weight percentage and density for PU foams

Denotation	Foam A	Foam B	Foam C
MWNT (wt%)	0	3	5
Density (kg/m^3)	270–320		

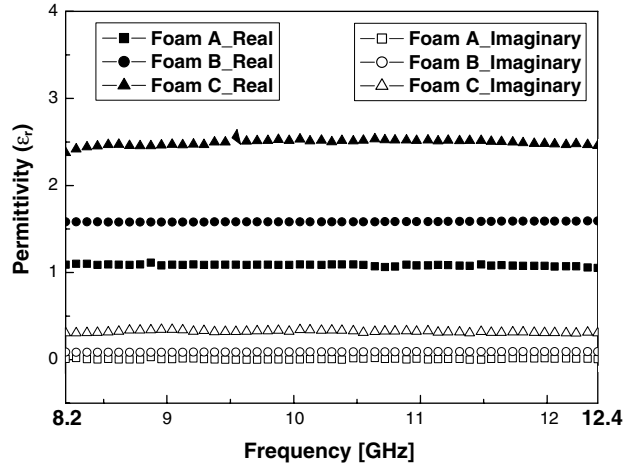

Fig. 7. Permittivity vs. frequency for PU foams.

The acquired permittivity characteristics of face sheets and forms were used for the calculation of the reflection loss for multi-layered sandwich structures.

4. Design and experimental results of electromagnetic wave absorbing sandwich structures

4.1. Design of electromagnetic wave absorbing sandwich structures

This section designs three types of RAS, namely, 3-, 4-, and 5-layered sandwich structures, based on the numerical simulation of reflection loss characteristics in X-band frequencies. The permittivity data of the face sheets and the fabricated foam cores, obtained in the previous chapter, and the theory of transmission and reflection in a multi-layered medium were used for the calculation. Our design parameters include the variation of layer sequence and the thickness variations of each layer. We selected three kinds of RAS which show good absorbing capacity among many calculated cases.

We set up some design restrictions: (1) Foam core(s) should be laminated as middle layer(s); (2) Foam cores should be thicker than face sheets; (3) The CFRP face sheet should be the last layer for reflective function so that no electromagnetic wave can be penetrated into the back side of the RAS. With these requirements, the optimal layer sequence and the thicknesses of each layer have been searched by intuition and trial and error (exhaustive search). The design goal was set to good reflection loss characteristics in the matching center frequency 10–10.5 GHz.

The design and calculation of reflection loss characteristics for 3-layered sandwich structures were performed as follows: the CB5 and CB6 face sheets having little dielectric loss terms were used as the 1st layer face sheet to reduce direct reflection at the 1st layer. Foam C that has large permittivity among three foams core was used as the 2nd layer. CFRP face sheet was used as the last layer. The reflection loss characteristics have been simulated for various thicknesses of the face sheets and the foam core. More specifically, the thickness ranging from 0.5 to 2.0 mm at an interval of 0.1 mm was tested for the face sheet and 20-times wide range of thickness was examined for the core.

The calculation of reflection loss characteristics for 4-layered and 5-layered sandwich structures was carried out in a similar way. For the case of 4-layered sandwich structures, the CB8 face sheet was added between Foam C layer and CFRP face sheet of 3-layered sandwich structures. For the case of 5-layered sandwich structures, Foam C was added between the CB8 face sheet and the CFRP face sheet of 4-layered sandwich structures. Particularly, 5-layered sandwich structures were similar to structures of Jaumann absorber [6].

Fig. 8 shows three cases of sandwich structures with good matching characteristics in the center frequencies 10–10.5 GHz. Case 1, Case 2 and Case 3 are the models of three-, four- and five-layered sandwich structures, respectively. Table 2 shows 10-dB absorbing bandwidth and matching thickness for each case. Note that 10-dB absorbing bandwidth means the frequency bandwidth having over 90% reflection loss characteristics. The performance of Case 1 was similar to that of Case 2. Case 3 shows better characteristics than Case 1 or Case 2 in 10-dB bandwidth.

4.2. Fabrication of EM wave absorbing sandwich structures

The designed specimens, Case 1, Case 2, and Case 3, were fabricated. First, face sheets and foam cores for each case were fabricated. Second, these were cut in thickness of each case. The width and length of these were 150×150 mm for measuring with the free space technique. Finally, after cutting face sheets and foam cores and bonding them using adhesive film, they were cured in the autoclave for 2 h at 3 atm, 120 °C. Fig. 9 shows the front view and side view for fabricated specimens of EM wave absorbing sandwich structures.

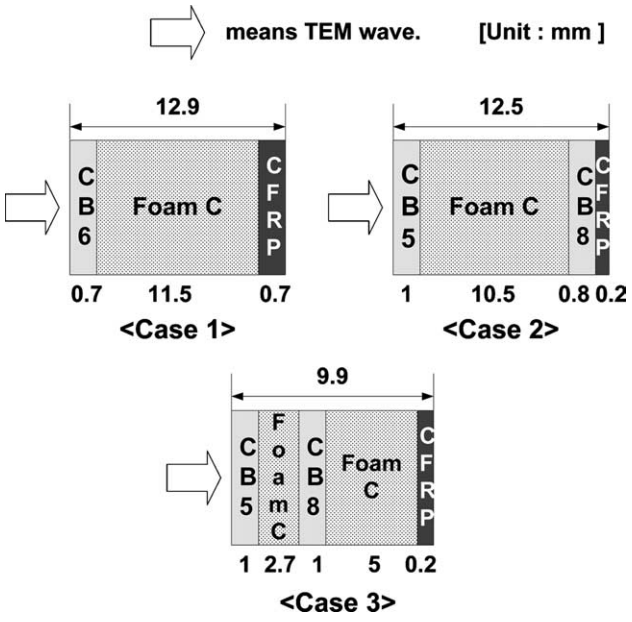

Fig. 8. Layer sequence and thickness of simulation models.

Table 2
Absorbing bandwidth and matching thickness for sandwich structures

	10-dB Bandwidth (GHz)	Matching thickness (mm)
Case 1	1.4 (9.7–11.1)	12.9
Case 2	1.2 (9.6–10.8)	12.5
Case 3	3 (8.7–11.7)	9.9

4.3. Measurement of reflection loss for fabricated specimens

The free space technique system for measuring reflection loss of TEM (transverse electromagnetic) wave are shown in Fig. 10. This system consists of a pair of spot-focusing horn lens antennas, a sample holder, HP 8510C network analyzer and a computer for data acquisition. The width and length of aluminum table are 1.83×1.83 m and the standard sizes of sample specimens for holder are 150×150 mm. The spot-focusing horn lens antennas for minimizing diffraction effects, the through-reflect-line (TRL) calibration technique and the time domain gating feature of HP 8510C network analyzer for minimizing multiple reflection were used in this system [14,15].

Figs. 11–13 show the simulation and experimental results for each case. All the experimental results show that the center frequencies were shifted a little from the theoretical predictions. However, the overall reflection loss behaviors were predicted very well for Case 1 and Case 2. For Case 3, the absorbing capacity in the center frequency decreased about 20 dB ($-42 \rightarrow -20$ dB). There were little differences between the simulation and experimental results for all three cases in the 10-dB absorbing bandwidths.

The discrepancy between the simulated results and the experimental ones can be caused by several factors, such as error in fabrication of specimens and measurement of permittivity and reflection loss. The error in fabrication comes from insufficient cutting accuracy and the insertion of adhesive films used in second bonding between face and core. The thickness of adhesive films was not considered in the simulations. Thereafter, we investigated the reflection loss characteristics of the sandwich structures according to the thickness of the adhesive film. The film has no dielectric loss so that the imaginary permittivity is assumed zero. The simulation was conducted assuming the thickness of the film as from 0.01 to 0.05 mm. The conclusion is that the insertion of the film had little effect on the reflection loss of the RAS in terms of the change of center frequency and absorbing bandwidth. Measurement errors can be caused by several problems such as misalignments for perpendicular penetration of incident wave and external noises during measurement.

4.4. Reflection loss characteristics for layer thickness variation of Case 1

We simulated the reflection loss characteristics considering the thickness variation error in fabrication. Fig. 14 shows reflection loss changes of Case 1 with ±10% in thickness of 1st layer, the CB6 face sheet. The thickness decrease made little increase in center frequency, while the increased thickness caused a little

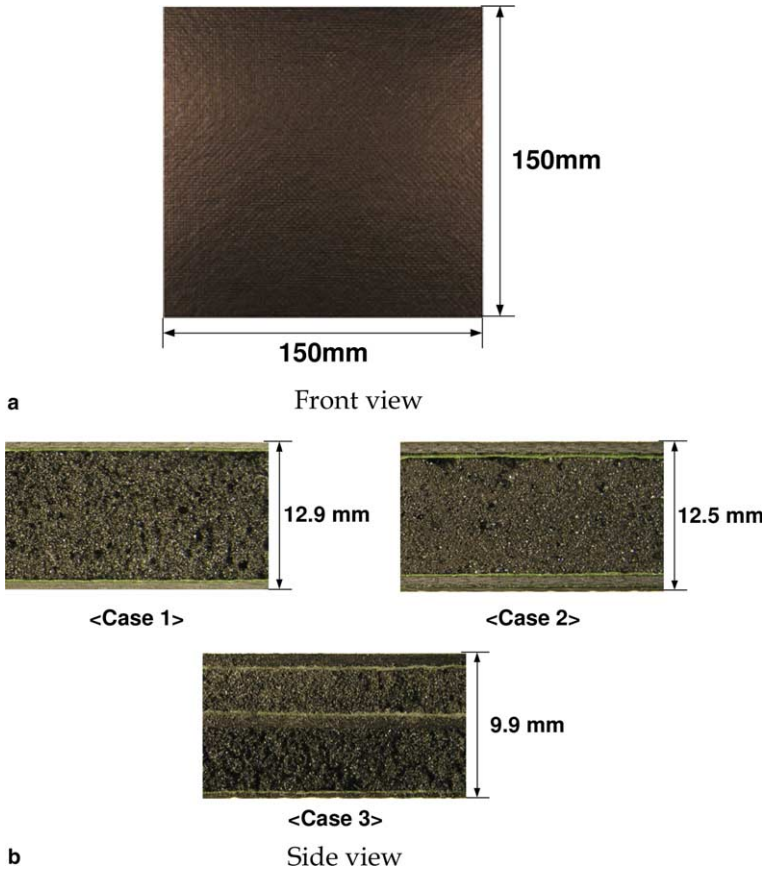

Fig. 9. Fabricated specimens of EM wave absorbing sandwich structures.

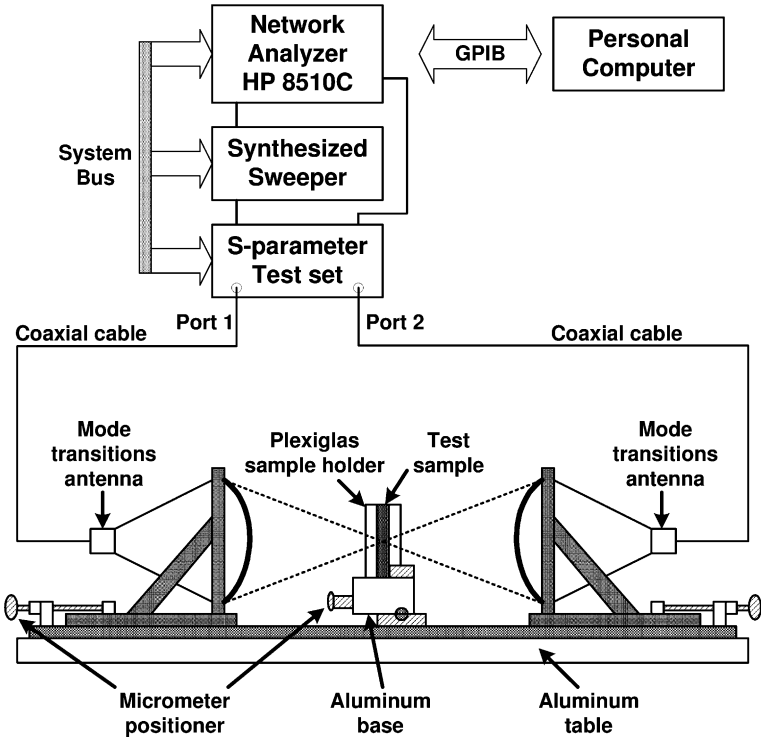

Fig. 10. Free space measurement system.

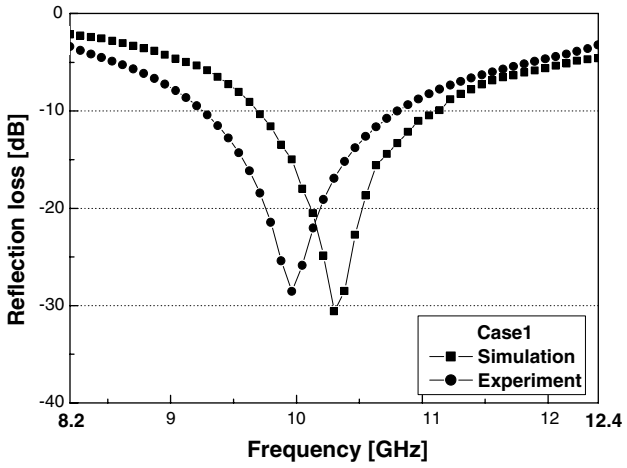

Fig. 11. Refection loss of Case 1 vs. frequency for simulation and experiment.

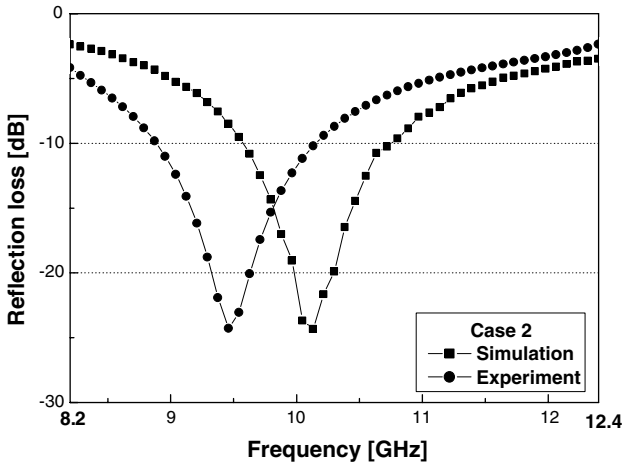

Fig. 12. Refection loss of Case 2 vs. frequency for simulation and experiment.

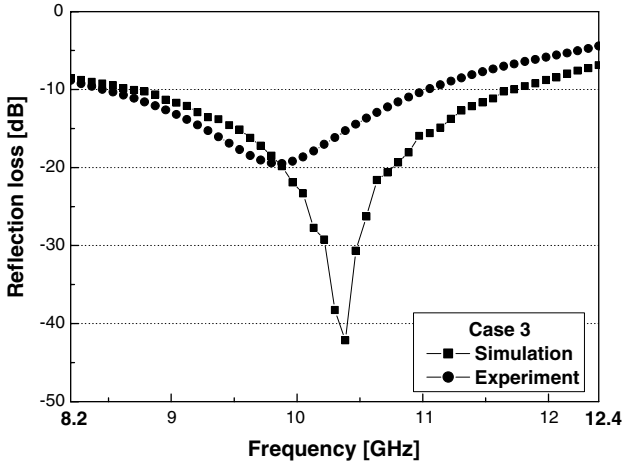

Fig. 13. Refection loss of Case 3 vs. frequency for simulation and experiment.

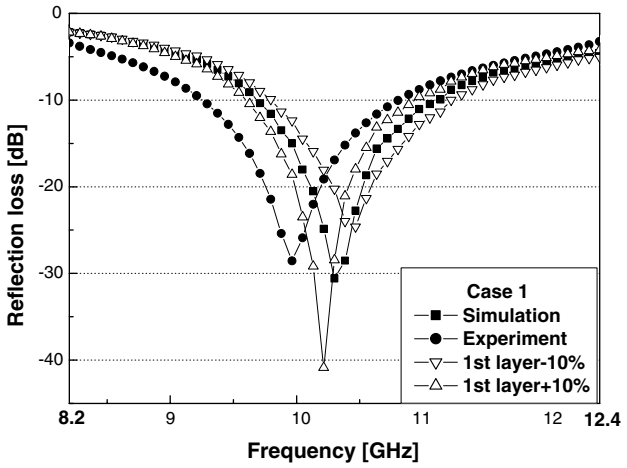

Fig. 14. Refection loss of Case 3 vs. frequency with 1st layer thickness variation.

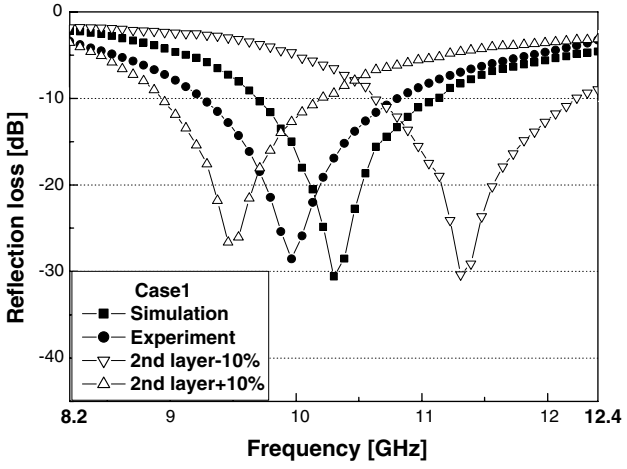

Fig. 15. Refection loss of Case 3 vs. frequency with 2nd layer thickness variation.

decrease of center frequency in the graph. But the variation of the center frequency is not enough to explain experimental result. Fig. 15 shows reflection loss changes with ±10% in thickness of 2nd layer, the Foam C core. There were similar reflection loss changes, but the variations of the center frequency were comparable with the experimental data. Because the CFRP face sheet was used as the backside of absorber, there were no reflection loss changes with thickness variation of the CFRP.

5. Conclusions

In this paper, we designed and fabricated the sandwich type RAS in the X-band frequencies. As conductive fillers such as carbon black and MWNT were added to composite face sheets and polyurethane foam

core, the absorbing capacity of RAS were efficiently increased. It is well known that sandwich construction also improves the mechanical stiffness of RAS.

Glass fabric/epoxy composites containing conductive carbon black and carbon fabric/epoxy composites showing shielding characteristics like conductor were used as the face sheets. Foam cores with isotropic electromagnetic properties were selected. Multi-walled carbon nanotube was added to the polyurethane foam to fabricate symmetric sandwich structures in thickness. The permittivity of these specimens was measured using the transmission line technique.

The reflection loss characteristics for multi-layered sandwich structures were calculated using the theory of transmission and reflection in a multi-layered medium and permittivity of specimens. Three cases of multi-layered sandwich structures were selected and fabricated. Their reflection losses in the X-band were measured using the free space technique. Experimental results compared with calculated ones showed generally the lower shift of 0.3–0.6 GHz in the matching center frequency, however the overall behavior of the reflection losses were predicted well such as 10-dB absorbing bandwidth. The little shift characteristics of reflection losses might be caused by errors in fabrication, measurement and so on.

For further the performance enhancement of RAS, the optimal design shall be exploited with more precise fabrication techniques. In addition, the multi-disciplinary design methodologies should be studied for practical applications of the sandwich type RAS.

Acknowledgment

This research was performed for the Smart UAV Development programs funded by the Ministry of Science and Technology of Korea.

References

[1] Oh JH, Oh KS, Kim CG, Hong CS. Design of radar absorbing structures using glass/epoxy composite containing carbon black in X-band frequency ranges. Composites Part B 2004;35:49–56.
[2] Vinoy KJ, Jha RM. Radar absorbing materials from theory to design and characterization. Boston: Kluwer Academic Publishers; 1996.
[3] Du JH, Sun C, Bai S, Su G, Ying Z, Cheng HM. Microwave electromagnetic characteristics of a microcoiled carbon fibers/paraffin wax composite in Ku band. J Mater Res Soc 2002;17(5):1232–6.
[4] Luo X, Chung DDL. Electromagnetic interference shielding using continuous carbon-fiber carbon-matrix and polymer-matrix composites. Composites Part B 1999;30:227–31.
[5] Das NC, Khastgir D, Chaki TK, Chakraborty A. Electromagnetic interference shielding effectiveness of carbon black and carbon fibre filled EVA and NR based composites. Composites Part A 2000;31:1069–81.
[6] Du Toit LJ. The design of Jauman absorbers. IEEE Antennas Propag Mag 1994;36(6):17–25.
[7] Munk BA. Frequency selective surfaces: theory and design. New York: Wiley; 2002.
[8] Internet site, Visby Class corvette; 2003. Available from: <http://www.kockums.se/>.
[9] Kim DI, Ahn YS, Chung SM. A study on development of high performance microwave absorbers in wide-band type for radar. J Korean Inst Navig 1991;15(1):1–9.
[10] Hayt WH, Buck JA. Engineering electromagnetics. McGraw-Hill; 2001.
[11] Chew WC. Waves and fields in inhomogeneous media. Van Nostrand Reinhold; 1990.
[12] Vinson JR. The behavior of sandwich structures of isotropic and composite materials. Technomic Publishing Company; 1999.
[13] Lin MS, Chen SH. Plane-wave shielding characteristics of anisotropic laminated composites. IEEE Trans Electromag Comp 1993;35(1):21–7.
[14] Ghodgaonkar DK et al. Free-space measurement of complex permittivity and complex permeability of magnetic materials at microwave frequencies. IEEE Trans Instrum Meas 1990;39:387–94.
[15] Seo IS, Chin WS, Lee DG. Characterization of electromagnetic properties of polymeric composite materials with free space method. Compos Struct 2004;66(1–4):533–42.